Synchronous late Pleistocene extensional faulting and basaltic volcanism at Four Craters Lava Field, central Oregon, USA

Benjamin H. Mackey[1,*], Samuel R. Castonguay[2,†], Paul J. Wallace[2], and Ray J. Weldon[2]
[1]*Department of Geological Sciences, University of Canterbury, PB 4800, Christchurch 8140, New Zealand*
[2]*Department of Geological Sciences, 1272 University of Oregon, Eugene, Oregon 97403, USA*

ABSTRACT

Central Oregon (northwestern USA), where northern Basin and Range extension diminishes in magnitude across the High Lava Plains, exhibits widespread extensional faulting and Quaternary volcanism, yet the relations between the processes are complex and chronology is poorly constrained. Here we use cosmogenic ^{3}He exposure dating of basalt lava flows to quantify the timing of normal faulting and emplacement of a lava field on the margins of pluvial Fort Rock Lake. The northwest-trending Christmas Valley fault system displaces High Lava Plains volcanic rocks, forming an ~3-km-wide graben that transects the eastern Fort Rock Basin. A portion of the western edge of the graben is marked by a normal fault displaying flexural shear folding with a prominent vertical hinge crack, called Crack in the Ground. Lava flows of the Four Craters Lava Field flowed into this crack. Exposure dating of the Four Craters Lava Field, on the eastern flank of the older Green Mountain shield volcano, indicates an emplacement age of 14 ± 1 ka. We dated Green Mountain basalt exposed in the walls of the crack (the fault wall), which also yielded exposure ages of 14 ± 1 ka. The similar ages suggest that substantial crack opening occurred at about the same time the Four Craters lava was emplaced. These data indicate a period of synchronous normal faulting and dike-fed cinder cone activity emanating from a fault-parallel fissure ~2 km northeast of the crack ca. 14 ka, with minimal displacement since.

INTRODUCTION

Cinder cones and associated basalt flows are common in extensional settings, and typically form along fissures (e.g., Tibaldi, 1995). Central Oregon (northwestern USA) has a complex network of extensional faults and lineaments (Pezzopane and Weldon, 1993) associated with hundreds of cinder cones (Weldon et al., 2003). Although the faults and volcanic features have been studied independently, the absence of any historic eruptions means that the nature and timing of how these normal faults interact with basaltic volcanism is largely unconstrained. Beyond the implications for the tectonic evolution of central Oregon, and general interactions between faulting and volcanism, there is a need to constrain the volcano-tectonic behavior for hazard prediction.

Although central Oregon has many Quaternary volcanic features, few have absolute ages. Most geochronology has focused on Tertiary and early Pleistocene basalt flows, rhyolite domes, and ash-flow tuffs of the High Lava Plains, and how they may relate to Yellowstone plume migration or the evolution of Newberry Volcano (e.g., Jordan et al., 2004). Late Pleistocene and Holocene lava flows can be challenging to date (Sims et al., 2007) because they are generally too young to have accumulated enough radiogenic ^{40}Ar for ^{40}Ar/^{39}Ar dating. Furthermore, finding suitable charcoal under lava flows for radiocarbon dating can be difficult in poorly vegetated desert environments (Sherrod et al., 2012), and frequently requires mechanical excavation (e.g., Kuntz et al., 1986). Cosmogenic ^{3}He has proven useful in dating young lava flows in the western U.S., particularly in the high deserts, where weathering and erosion of lava are minimal and cosmogenic nuclide production rates are high (e.g., Cerling and Craig, 1994; Licciardi et al., 1999; Ely et al., 2012).

Here we focus on the nature and timing of interaction between the Four Craters Lava Field and the Crack in the Ground fault in central Oregon. Lava at the southwest margin of the lava field flowed into, and abuts, the Crack in the Ground fault, an extensional fissure in older basalt produced by normal faulting. The location is well suited to study the timing of lava emplacement and extensional faulting.

In this paper we first describe the regional setting, Four Craters Lava Field, and the adjacent Crack in the Ground fault. We then outline our sampling strategy for cosmogenic ^{3}He exposure dating to determine the timing and nature of the interaction between the lava and fault. We present results of cosmogenic ^{3}He exposure dating and interpret these to unravel the interaction between the Crack in the Ground fault and the Four Craters Lava Field.

FOUR CRATERS LAVA FIELD

The propagation of Basin and Range extension into the Oregon High Lava Plains (Fig. 1) generates a complex network of largely en echelon normal faults (Walker and MacLeod, 1991; Pezzopane and Weldon, 1993; Crider, 2001). This zone of extension is bounded by the Brothers fault zone to the north and the Walker Rim fault zone to the west, and coincides with pervasive Neogene volcanism across the Oregon High Lava Plains. Beyond stratigraphic and crosscutting relations, or relative dating based on appearance (e.g., degree of weathering or vegetation), there is limited information on the timing of faulting or Pleistocene volcanic activity, and how faulting might relate to periods of volcanism.

Fort Rock Basin is in a band of northwest-striking faults between Summer Lake and Newberry Volcano (Fig. 1). The closed basin contained the ~60-m-deep pluvial Fort Rock Lake during the last glacial maximum (Allison, 1979), with paleoshorelines preserved to ~1350 m elevation. The basin hosts a range of phreatomagmatic Quaternary volcanic features (Heiken, 1971; Brand and Heiken, 2009). The Christmas Valley fault system bisects the eastern arm of the Fort Rock Basin, forming a north-northwest–trending graben, creating a depression in the older Green Mountain basaltic shield and the playa delineated by the Crack in the Ground fault on the northwest and the Viewpoint fault on the southeast (Fig. 2).

The 19 km^2 Four Craters Lava Field (Fig. 3) is within this graben, and covers a part of the

*ben.mackey@canterbury.ac.nz
†Present address: Geology Department, University of Wisconsin-Eau Claire, Eau Claire, Wisconsin 54702, USA

Geosphere; December 2014; v. 10; no. 6; p. 1247–1254; doi:10.1130/GES00990.1; 5 figures; 2 tables.
Received 10 October 2013 ♦ Revision received 11 July 2014 ♦ Accepted 8 October 2014 ♦ Published online 12 November 2014

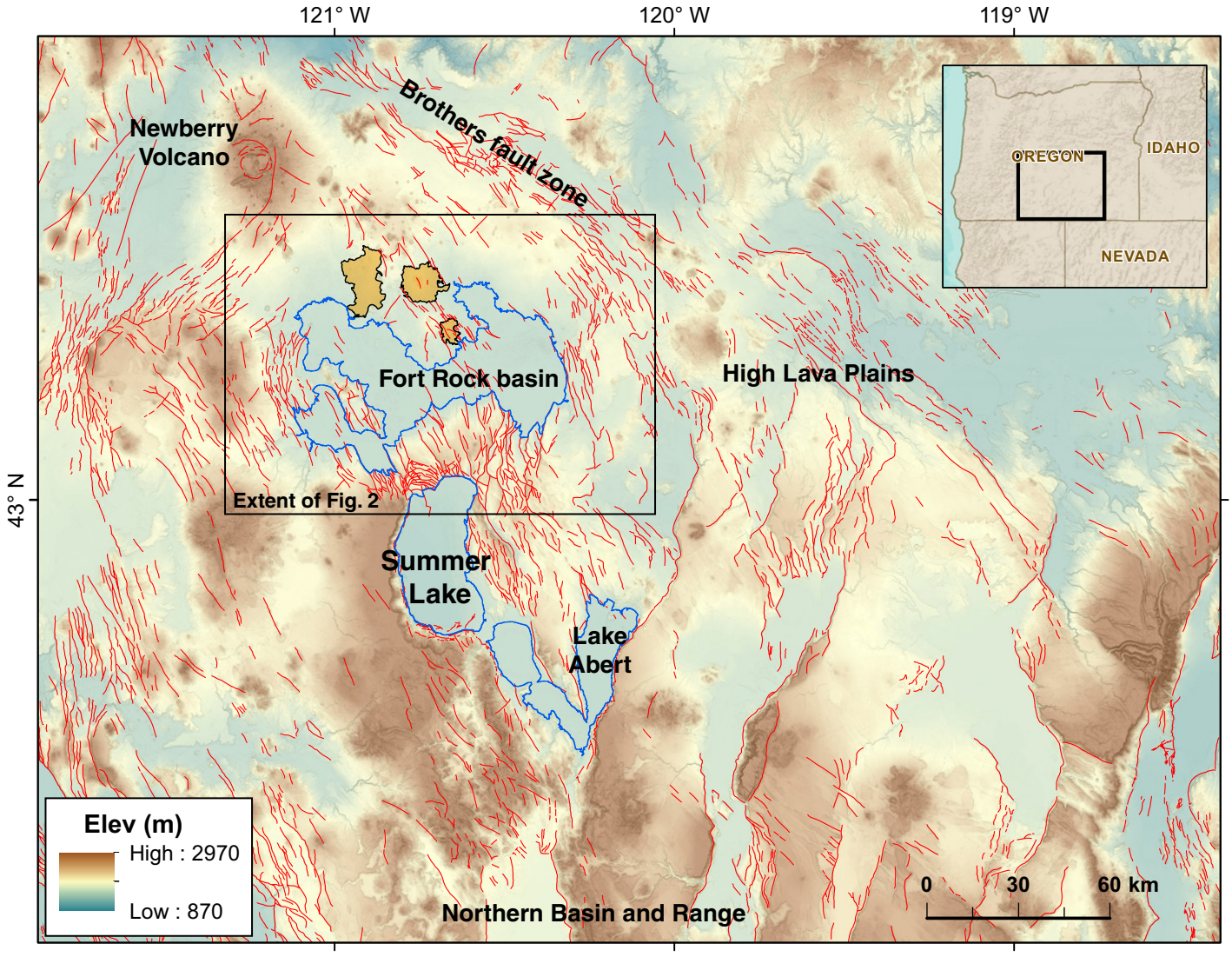

Figure 1. Location of study area in central Oregon (inset). Red—Quaternary faults from Weldon et al. (2003). Blue line is 1335 m contour line, showing the approximate extent of pluvial lakes in the late Pleistocene. Orange areas are the late Pleistocene basalt fields described in text (see Fig. 2).

eastern flank of the older 25-km-diameter Green Mountain shield volcano (740 ± 59 ka; Jordan et al., 2004). The Crack in the Ground fault, a normal fault downthrown to the northeast, delineates a section of the southwest boundary of the Four Craters Lava Field. The Four Craters Lava Field had not been dated previously, but has been estimated to be Holocene in age due to the fresh appearance of the lava and sparsely vegetated flow surface (Peterson and Groh, 1963; Walker et al., 1967; Walker and MacLeod, 1991; Meigs et al., 2009). The Four Craters Lava Field's four cinder cones are aligned N33°W and presumably were controlled by a fault-parallel fissure ~2 km northeast of the Crack in the Ground fault (Fig. 3). Two northwest-striking faults project partially across the lava field and have been interpreted to indicate some postemplacement extension, with activity assumed to be Holocene in age (Pezzopane and Weldon, 1993). The East lava field, 6 km northwest of the Four Craters Lava Field, has a similar morphologic appearance based on its lack of soil, vegetation, and weathering, and has been assumed to be similar in age to the Four Craters Lava Field (Fig. 2) (Peterson and Groh, 1963). The Devil's Garden lava field, also undated, is 5 km west of the East lava field (Fig. 2).

The Crack in the Ground fault is a normal fault that has flexurally sheared upper layers of Green Mountain basalt, forming a prominent tension crack in the upper hinge (Peterson and Groh, 1963, 1964). The crack is open for ~3 km, and can reach 20 m in depth (Peterson and Groh, 1964). The fault averages 8 m of vertical separation (but can reach 13 m), although much of this displacement is accommodated by the flexural shearing forming a hanging-wall monocline across the upper Green Mountain lava. Similar features in Iceland have been attributed to friction on the fault plane at depth (Gudmundsson et al., 1993). The vertical offset across the two sides of the crack reaches a maximum of 4 m (Fig. 4). The Crack in the Ground fault emerges from the dry sediments in the bed of pluvial Fort Rock Lake, cuts across the Green Mountain basalt flows, continues northwest to bound a section of the Four Craters Lava Field, then continues along strike across the northeast flank of Green Mountain (Fig. 2). In places the fault has opened cleanly, and opposite fault walls clearly

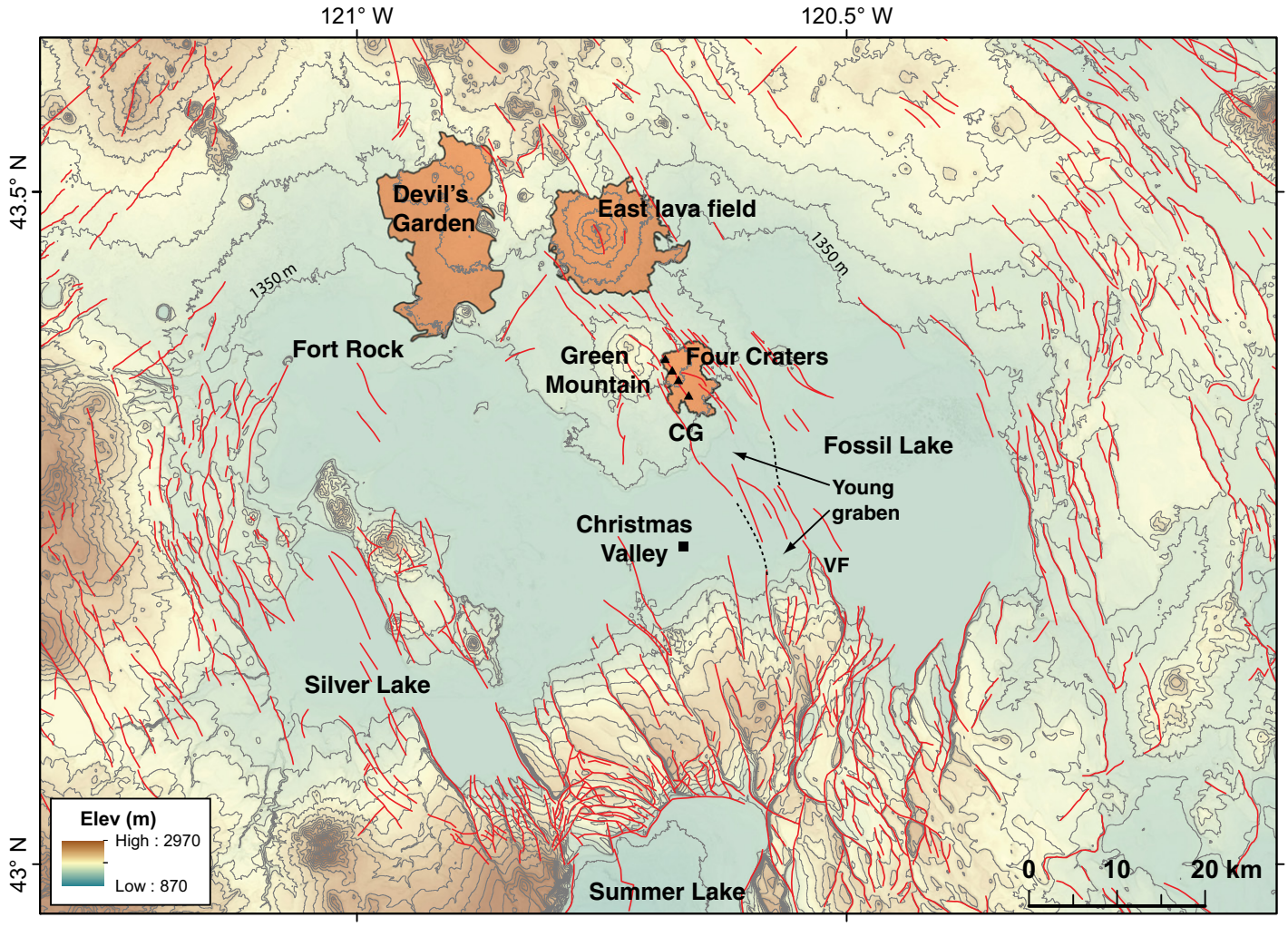

Figure 2. Location of Four Craters Lava Field on the eastern flank of the Green Mountain shield volcano; black triangles mark the four cinder cones. Fault database is from Weldon et al. (2003). Orange areas are late Pleistocene lava flows. Dashed black lines highlight the young graben bound by the Crack in the Ground fault (CG) on the west and the Viewpoint fault (VF) to the southeast. Contour interval is 50 m. 1350 m contour (labeled) is approximate highstand of pluvial Fort Rock Lake.

match, indicating no post-opening rockfall or modification of the crack wall (Fig. 4), whereas in other sections the fault walls have collapsed into the crack. A portion of the Four Craters lava abuts and flowed into the Crack in the Ground fault (Fig. 3), a relationship indicating that the flow must postdate the Crack in the Ground opening (Peterson and Groh, 1964).

METHODS AND SAMPLING STRATEGY

To establish the age distribution of the Four Craters Lava Field, we took 13 samples of basalt from the surface of the lava flows (Fig. 3), including at least 1 sample from flow lobes emanating from each of the 4 cones. Samples were obtained by chipping off the surface layer of rock with a hammer and chisel. We generally sampled flat surfaces that required minimal topographic shielding correction, avoiding locations affected by lava collapse, or zones of tephra deposition proximate to the cinder cones (Fig. 3). The presence of stretched vesicles indicated that we sampled original lava surface and suggests minimal erosion. We were unable to locate a suitable cosmic ray–shielded sample from the Four Craters Lava Field, as discussed in the following. In addition, we took a surface sample from an inflation feature on Green Mountain basalt (GM-1) and two samples from the southern margin of the East lava field, 6 km northwest of the Four Craters Lava Field (Fig. 2).

To constrain the timing of activity of the Crack in the Ground fault, we sampled the walls of the crack in 4 places along a 600-m-long section of the fault (Figs. 3 and 4). Three samples were taken in Green Mountain lava, and a fourth came from a smaller crack in Four Craters lava. Care was taken to ensure samples were obtained where opposing fault walls identically matched (Fig. 4) and had not been modified by block collapse into the crack or by erosion. Samples from the crack wall were taken at least 3 m below the original ground surface to ensure minimal accumulation of cosmogenic ^{3}He before exposure of the sample when the crack opened.

Samples from the crack interior required extensive correction for topographic shielding, as they were located on vertical walls with additional shielding from the opposite fault wall (e.g., Dunne and Elmore, 2003). We took 20–30 measurements of the skyline geometry for each sample using a hand-held laser rangefinder, with an internal digital compass and inclinometer, and determined the topographic shielding factor using the CRONUS shielding calculator

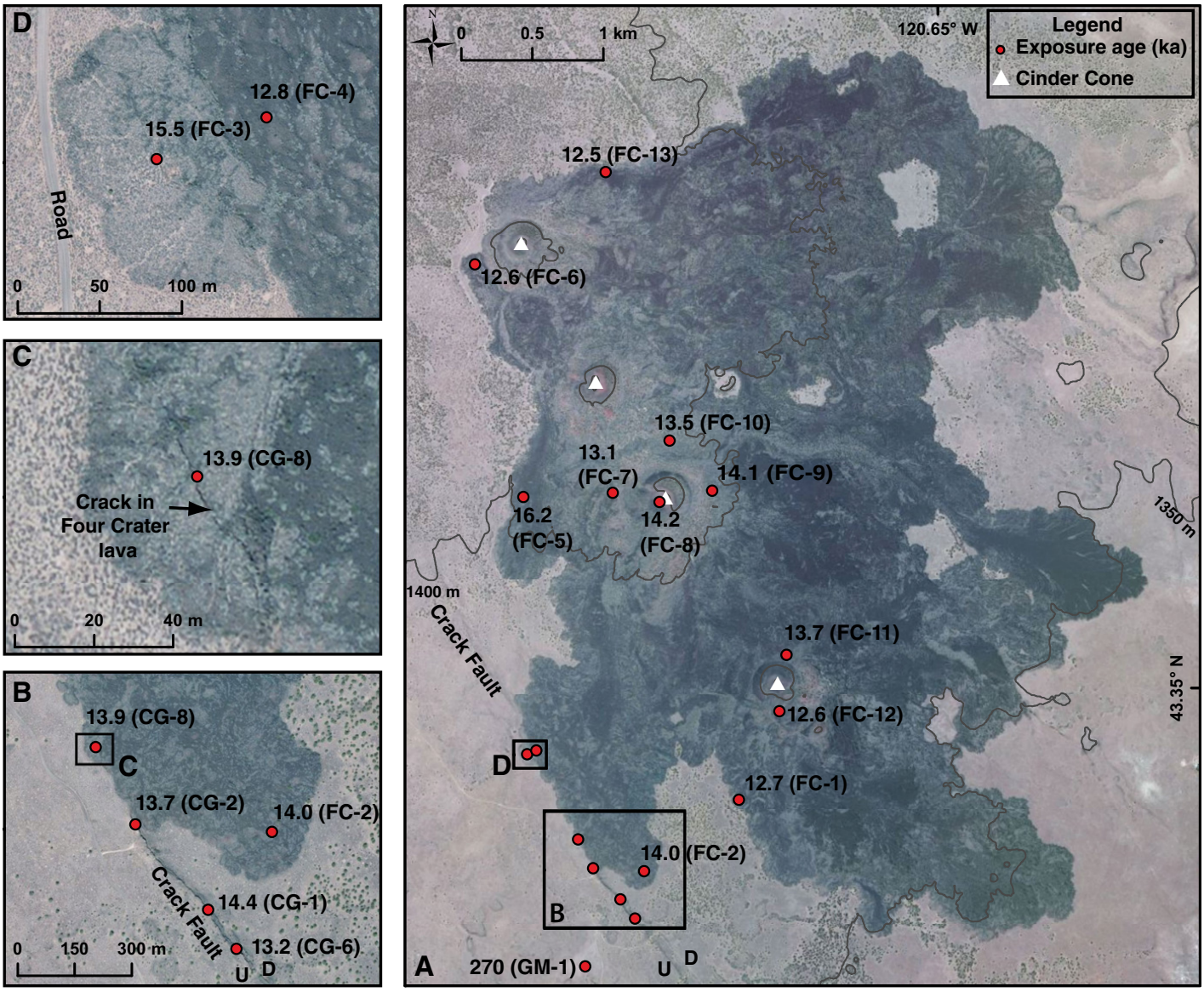

Figure 3. Aerial view of Four Craters Lava Field and Crack in the Ground fault (Crack fault), showing sample (FC—Four Craters Lava Field; CG—Crack in the Ground; GM—Green Mountain basalt) locations and exposure ages. Contour interval is 50 m. White triangles mark the four cinder cones. Aerial imagery is from Bing Maps.

(Balco et al., 2008). Cosmogenic exposure measurements within the crack represent an extreme example of topographic shielding (Dunne and Elmore, 2003), with as much as 60% of cosmogenic rays blocked compared to an unobstructed surface sample. Studies have questioned whether conventional shielding calculations, designed for distant skyline geometry, are appropriate for these extreme cases (e.g., Matmon et al., 2005; Balco et al., 2008; Rinat et al., 2014). We do not account for effects where the incoming cosmic ray flux may not be fully blocked, such as where the upper corner of shielding cliffs has a length scale comparable to the attenuation length of cosmic rays in rock. Recognizing the complicated geometry of the Crack in the Ground samples, and uncertainty whether cosmogenic production rate scaling equations are applicable to subvertical surfaces, we assigned a conservative error to the topographic shielding factor of ±0.05 (unitless).

Given the ca. 740 ka age of the Green Mountain basalt, we obtained a shielded sample (CG-7) from a small cave adjacent to the Crack in the Ground that was ~4 m below the original ground surface. This sample is needed to correct for noncosmogenic sources of ^{3}He as described in the following.

Each sample was cut to a thickness of 3 cm, crushed in a jaw crusher, and sieved. Olivine phenocrysts in both the Green Mountain and Four Craters lavas were generally small (<0.5 mm diameter) and sparse; 1–2 kg of rock was required to get sufficient sample mass (~0.5 g). Phenocrysts from the 250–450 µm fraction were separated using standard magnetic and heavy liquid techniques and sonicated in ~5% HF:HNO_3 to remove surface alteration. We checked each sample under a binocular microscope to remove any phenocrysts with adhering groundmass. Aliquots of cleaned olivine were crushed by hand using a mortar and pestle and wet sieved to 37 µm to breach any melt inclusions and release their mantle gasses, a potential source of noncosmogenic ^{3}He. The olivine

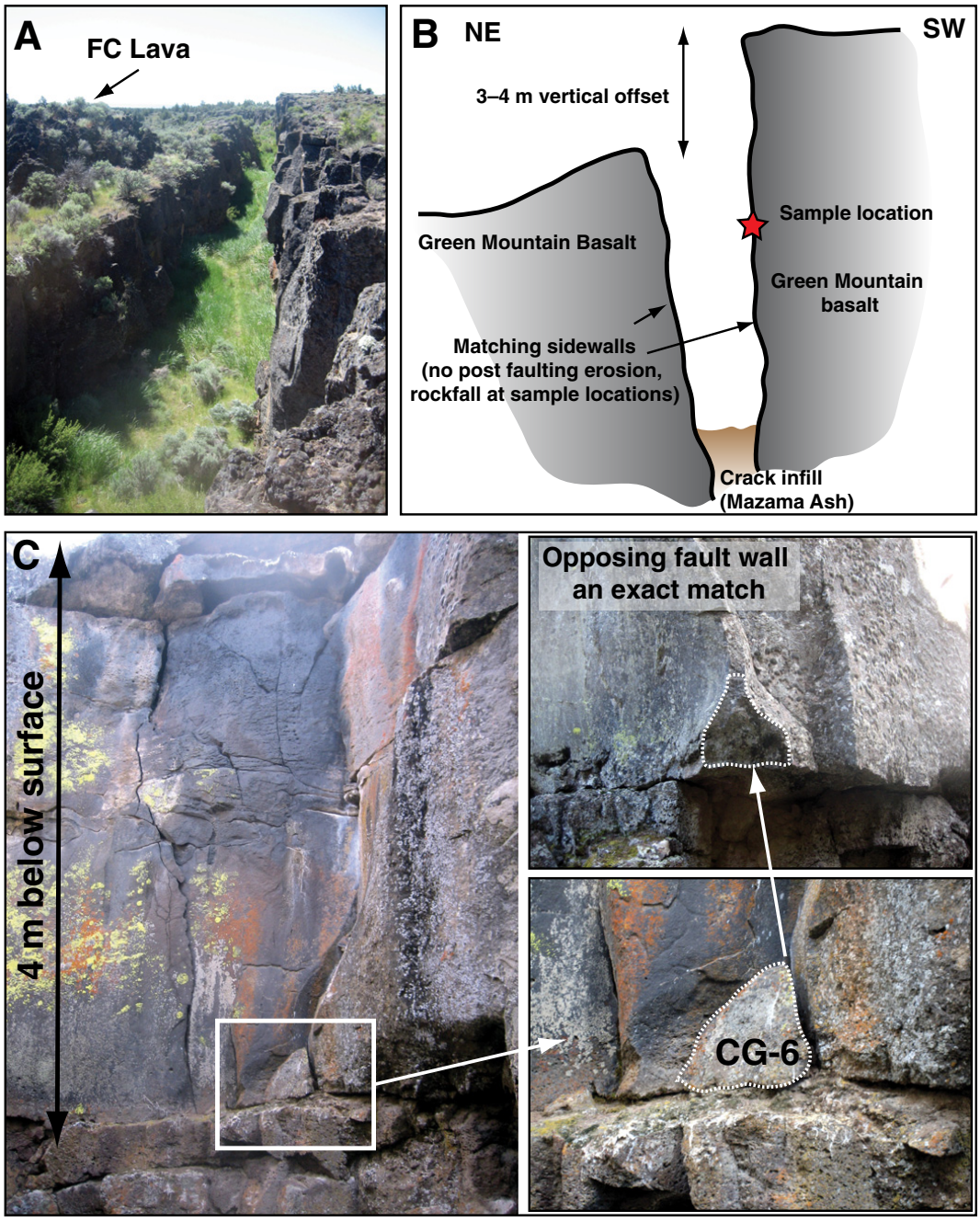

Figure 4. (A) View of Crack in the Ground (CG) fault looking to southeast. Downthrown side is to the left. The margin of the Four Craters Lava Field (FC) lava is just short of the CG fault in this location; crack is ~8 m deep and 3–4 m wide; grass in base is growing on reworked Mazama ash. (B) Cross section showing representative sample location in the CG fault. All samples were taken from the footwall (southwest wall) of the fault. (C) Location of sample CG-6. The triangular facet has an identical matching feature on the opposing fault wall.

phenocrysts contained abundant dark colored inclusions, likely Cr spinel (e.g., Hart et al., 1984), or solidified glass inclusions.

The olivine powder was wrapped in Al foil and heated to 1300 °C under vacuum. ^{3}He and ^{4}He gas was measured on a MAP noble gas mass spectrometer at the Caltech Noble Gas Laboratory following the methods described in Amidon and Farley (2011). We calculated the ^{3}He exposure age using the CRONUS ^{3}He exposure age calculator (Balco et al., 2008; Goehring et al., 2010), using the scaling scheme of Desilets et al. (2006). Calculations assumed a neutron attenuation length of 160 g/cm^{2}, and a minimal background erosion rate of 0.1 mm/k.y.

In a sample of olivine there are multiple potential components of ^{3}He. These consist of ^{3}He produced by cosmic rays, mantle-derived (magmatic) ^{3}He trapped in inclusions within the phenocryst, and nucleogenic ^{3}He (e.g., via neutron capture on ^{6}Li). The conventional approach to isolate cosmogenic ^{3}He (e.g., Kurz, 1986) uses the relation

$$^{3}\mathrm{He}_{c} = {}^{3}\mathrm{He}_{f} - {}^{4}\mathrm{He}_{f} \times (^{3}\mathrm{He}/^{4}\mathrm{He})_{mag}, \quad (1)$$

where ^{3}He$_{c}$ denotes cosmogenic ^{3}He; ^{3}He$_{f}$ and ^{4}He$_{f}$ are the total concentrations of each He isotope measured by fusion of olivine powder; and $(^{3}\mathrm{He}/^{4}\mathrm{He})_{mag}$ is the magmatic (mantle) ratio (measured ratio relative to the ratio in air: 1.4 × 10^{-6}, commonly denoted R/R_A). As shown in Table 1, there is considerable variance in ^{4}He concentrations from the Four Craters Lava Field samples. Higher than expected concentrations of ^{4}He are possibly attributable to

TABLE 1. HELIUM DATA FOR OLIVINE SAMPLES, CENTRAL OREGON

Sample*	Mass (g)	^{3}He (10^6 atoms/g)	±1σ	^{4}He (10^{12} at/g)	±1	R/R_A melt
FC-1	0.4075	4.30	0.26	0.05	0.003	56.9
FC-2	0.3233	4.73	0.28	0.05	0.003	61.4
FC-3	0.345	5.29	0.32	0.06	0.003	62.6
FC-4	0.2147	4.34	0.26	0.13	0.006	24.7
FC-5	0.3954	5.67	0.34	0.02	0.001	236.2
FC-6	0.3744	4.41	0.26	0.02	0.001	188.3
FC-7	0.3575	4.58	0.27	0.29	0.015	11.1
FC-8	0.2977	4.75	0.29	13.66	0.683	0.3
FC-9	0.3643	4.90	0.29	0.72	0.036	5.3
FC-10	0.275	4.70	0.28	0.48	0.024	7.6
FC-11	0.1309	4.62	0.28	0.72	0.036	4.9
FC-12	0.4627	4.22	0.25	0.14	0.007	21.8
FC-13	0.4766	4.37	0.26	0.15	0.007	22.5
ELF-1	0.1752	4.70	0.28	0.31	0.016	10.8
ELF-2	0.4425	4.25	0.25	0.07	0.003	45.7
GM-1	0.2083	95.8	5.75	5.60	0.280	13.1
CG-1	0.3446	2.44	0.15	0.07	0.003	26.2
CG-2	0.3296	2.34	0.14	0.03	0.001	60.6
CG-6	0.221	2.19	0.13	0.68	0.034	2.5
CG-8	0.4092	2.13	0.13	0.46	0.023	3.6
CG-7	0.0652	0.51	0.03	8.62	0.431	0.0

Note: R/R_A—measured He isotope ratio divided by the atmospheric He isotope ratio (R_A), 1.4×10^{-6}.
*FC—Four Craters Lava Field; ELF—East lava field; GM—Green Mountain basalt; CG—Crack in the Ground.

mineral phases containing high concentrations of U or Th either within or associated with the olivine that can generate ^{4}He through alpha decay. The ^{4}He concentrations enriched in radiogenic ^{4}He can generate erroneously young ^{3}He exposure ages if Equation 1 is used (Blard and Farley, 2008).

Given the variance in ^{4}He, for the samples from the Four Craters Lava Field we simply assume that all ^{3}He measured in the olivine is cosmogenic. There is potential for a minor component of residual mantle-derived and nucleogenic ^{3}He, but it is likely to be minor (1%–2%) given the relatively young age of the lava (Amidon and Farley, 2011), and the modest mantle R/R_A ratio of 8.83 ± 0.11 previously measured from this flow (Graham et al., 2009). If we apply Equation 1, the calculated ^3He_c ranges from 0% to 96% of the measured ^{3}He. For the samples from much older Green Mountain lava, where there is potential for significant nucleogenic ^{3}He accumulation, the concentration of ^{3}He measured in the cosmic ray–shielded sample was used to correct for any noncosmogenic ^{3}He (e.g., Margerison et al., 2005; Mackey et al., 2014).

RESULTS

The results of the ^{3}He exposure age dating are presented in Tables 1 and 2 and displayed geographically in Figure 3. Figure 5 shows the relative probability of ages for the Four Craters Lava Field, the Crack in the Ground wall, and the East lava field.

Assuming all measured ^{3}He is cosmogenic, the exposure ages of the Four Craters Lava Field samples range from 12 to 16 ka (Figs. 3 and 5), with a mean weighted age of 13.7 ± 0.3 ka. The two ages from the East lava field have a mean weighted age of 12.8 ± 0.5 ka.

At the site elevation (~1350 m), the cosmogenic ^{3}He production rate in olivine is ~370–390 atoms/g/yr, based on a scaling factor of 3.1–3.26 compared to the reference sea-level high-latitude production rate of 120 atoms/g/yr (Goehring et al., 2010). The shielded sample of Green Mountain basalt (CG-7) had a ^{3}He concentration of 0.51×10^6 atoms/g (Table 1), and we subtracted this concentration from the total ^{3}He concentration for each sample from Green Mountain basalt (Table 2).

We can compare the relative age of the Four Craters and Green Mountain basalts (14 and 740 ka respectively) relative to the ^{3}He concentration in the Green Mountain shielded sample (CG-7). A comparable shielded sample from Four Craters lava should have a noncosmogenic ^{3}He component of ~0.01×10^6 atoms/g, < 1% of the total measured ^{3}He in the Four Craters surface samples.

Age calculations for Crack wall in Green Mountain lava samples CG-1, CG-2, and CG-6 required significant topographic shielding corrections; the ages are 14.4 ± 1.9, 13.7 ± 1.8 and 13.2 ± 1.9 ka, respectively, with a mean weighted age of 13.8 ± 0.5 ka. The larger error (Table 2) is due to uncertainty we imposed due to the topographic shielding and subtraction of the shielded sample, yet the exposure ages from the Crack in the Ground fault wall are similar

TABLE 2. SAMPLE LOCATIONS IN OREGON AND EXPOSURE AGES

Sample	Description	Lat (WGS84)	Long (WGS84)	Elevation (m)	Topographic shielding	^3He_c (10^6 atom/g)	^{3}He production rate (atom/g/yr)	Age (ka)	±1σ
FC-1	FC flow	43.3417	–120.6642	1372	1.00	4.30	374	12.7	0.8
FC-2	FC flow	43.3369	–120.6721	1373	1.00	4.73	374	14.0	0.8
FC-3	FC flow	43.3440	–120.6827	1380	1.00	5.29	376	15.5	0.9
FC-4	FC flow	43.3442	–120.6819	1382	1.00	4.34	377	12.8	0.8
FC-5	FC flow	43.3602	–120.6840	1407	1.00	5.67	384	16.2	1.0
FC-6	FC flow	43.3748	–120.6891	1425	1.00	4.41	389	12.6	0.7
FC-7	FC flow	43.3607	–120.6763	1418	1.00	4.58	388	13.1	0.8
FC-8	FC flow	43.3603	–120.6722	1419	0.95	4.75	369	14.2	0.8
FC-9	FC flow	43.3612	–120.6677	1404	1.00	4.90	384	14.1	0.8
FC-10	FC flow	43.3642	–120.6716	1407	1.00	4.70	384	13.5	0.8
FC-11	FC flow	43.3510	–120.6606	1375	1.00	4.62	374	13.7	0.8
FC-12	FC flow	43.3474	–120.6610	1402	0.97	4.22	371	12.6	0.7
FC-13	FC flow	43.3810	–120.6781	1417	1.00	4.37	388	12.5	0.7
ELF-1	ELF flow	43.4262	–120.7200	1377	1.00	4.70	375	13.9	0.8
ELF-2	ELF flow	43.4375	–120.7917	1376	1.00	4.25	375	12.5	0.7
GM-1	GM Flow	43.3307	–120.6769	1377	0.99	95.79	371	272.0	16.0
CG-1	GM crack	43.3347	–120.6739	1365	0.40 ± 0.05	1.94	149	14.4	1.9
CG-2	GM crack	43.3369	–120.6765	1367	0.40 ± 0.05	1.84	149	13.7	1.8
CG-6	GM crack	43.3341	–120.6731	1364	0.38 ± 0.05	1.69	141	13.2	1.9
CG-8	FC crack	43.3387	–120.6779	1376	0.45 ± 0.05	2.13	169	13.9	1.7
CG-7	GM shield	43.3361	–120.6756	1362	0.00	NA	NA	NA	NA

Note: FC— Four Craters Lava Field; ELF—East lava field; GM—Green Mountain basalt; CG—Crack in the Ground. WGS84—World Geodetic system 1984 datum. ^3He_c is cosmogenic He; the GM samples are corrected for the shielded sample (CG-7). Cosmogenic ages were calculated on the CRONUS cosmogenic ^{3}He calculator using the DE scaling scheme of Desilets et al. (2006). Bulk density of basalt was 2.6 ± 0.1 g/cm^3. Age includes a self-shielding component of 0.976. NA—not applicable to shielded sample.

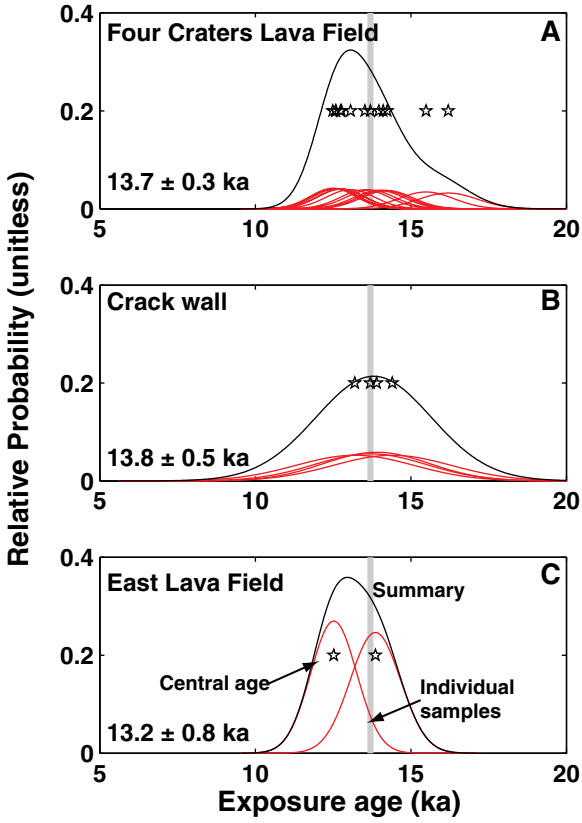

Figure 5. Combined relative probability estimate (unitless) for cosmogenic ages. Vertical gray line represents the weighted median age of the Four Craters surface exposure ages. Red lines are the Gaussian curve of each sample (±1σ), and black line is the sum of all curves. (A) Four Craters Lava Field. (B) Crack in the Ground fault wall. (C) East lava field.

to the surface exposure ages of the Four Craters lava. The sample from the small crack within the Four Craters lava (CG-8) has an exposure age of 13.9 ± 1.7 ka. The surface sample of Green Mountain lava has a ^{3}He exposure age of 272 ± 16 ka.

DISCUSSION

Timing of Volcanism

Cosmogenic ^{3}He exposure dating of the Four Craters Lava Field indicates that the flows were emplaced ca. 14 ka. There is no systematic variance across the different flows, suggesting that eruptions from the four vents were clustered in time, well below the resolution of ^{3}He exposure dating.

Two ages from the Four Craters Lava Field are older (samples FC-3, FC-5) than the majority of ages (Table 2; Fig 5), although they overlap within error. Although we have only two exposure ages from the East lava field, they are within error of the ages from the Four Craters field, suggesting that the two fields were active at a similar time. Our exposure age of an inflation feature on Green Mountain lava (ca. 270 ka) is significantly younger than the ^{40}Ar/^{39}Ar age of 740 ka for the same unit (Jordan et al., 2004). Given the age of the flow, there is potential for substantial erosion of the lava surface, which would render our exposure age a minimum estimate (e.g., Sims et al., 2007).

Timing of Crack Opening

The four exposure ages from the crack wall also are broadly similar (13.2 ± 1.9, 13.7 ± 1.8, and 14.4 ± 1.9 ka), despite spanning 600 m along the fault and each sample location having a different shielding geometry. There are two ways to interpret these data. The first is that the crack opened in one short episode to its current configuration, with little to no activity since. Alternatively, the crack may have opened incrementally over a longer period. In the second scenario, the initial topographic shielding would be severe, gradually reducing to its current geometry as the crack opened. A slow, prolonged opening over a longer period of time could generate an apparent exposure age of 14 ka due to suppressed cosmogenic production at the sample depths when the crack was barely open.

We favor the first interpretation, as the three samples from the main crack all have approximately the same exposure age. Were the crack to have opened incrementally over a much longer period of time, dating should produce a range of apparent exposure ages, due to the different evolution of shielding geometry at each sample site as the crack opened. The one crack sample from the small crack within the Four Craters lava (CG-8; Fig. 3C) has an exposure age (13.9 ± 1.7 ka) similar to samples from the primary crack (13.8 ± 0.5 ka) in the Green Mountain basalt, indicating that there has been minimal movement of the fault since the Four Craters lava was emplaced.

It is possible that the flexural shear fold in the upper layers of the Green Mountain basalt had some relief before 14 ka, and the faulting event ca. 14 ka finally caused the opening of the overlying Green Mountain lava across the fault. The stacked lava flows on the flank of the Green Mountain shield could have accommodated initial vertical movement through warping and flexure before eventually cracking with continued movement. The upper layers of sediment infilling the crack is from the Mount Mazama (Crater Lake) eruption (7.6 ka; Zdanowicz et al., 1999). Prior attempts to trench the floor of the Crack in the Ground revealed windblown basaltic sands and silts of unknown age below the Mazama ash, but no evidence of fault-related disturbance of the infilling sediment (R. Langridge, 2013, personal commun.). This indicates that the crack has been inactive since at least the early Holocene, and further supports our contention that the crack opened to its current configuration in a relatively short time period.

Direct dating of fault scarps has only been attempted a few times before, most commonly on large limestone normal faults where transects up exposed footwall faces can document repeated fault movements (e.g., Schlagenhauf et al., 2011; Akçar et al., 2012). Settings similar to the Crack in the Ground fault can be found in many basaltic landscapes where movement such as faulting or mass movement exposes a previously buried rock face, enabling paleoseismic investigations where there may be little depositional record.

Interaction Between Lava and Fault

A tongue of lava from the Four Craters Lava Field flowed into the Crack in the Ground; this is unequivocal field evidence that the crack predated or opened coeval with volcanic activity. The exposure ages of the Crack in the Ground wall and the lava field are identical within error (Fig. 5), indicating that opening of the Crack in the Ground and eruption of the Four Craters Lava Field occurred at a similar time. This is emphasized by the localized lobe of Four Craters lava that crosses the Crack in the Ground fault (Fig. 3C) and has minor crack development. An exposure age from a sample on the wall of this crack in Four Craters lava also has a surface exposure age of ca. 14 ka

(Table 2), similar to the other crack samples, despite the Four Craters Lava Field basalt being much younger than the Green Mountain basalt in the main part of the crack. We interpret this to reflect lava flow into and across the fault, followed by continued fault motion shortly after the flow solidified. Although the Crack in the Ground fault was active prior to eruption, the similar exposure ages of the lava flows and crack wall strongly imply that the crack opening was coincident with the emplacement of the Four Craters Lava Field.

CONCLUSION

We present new cosmogenic ^{3}He exposure dating results for the Four Craters Lava Field in central Oregon, which indicates that the field was emplaced ca. 14 ka. This time coincides with the exposure age of the adjacent Crack in the Ground normal fault, indicating that the volcanic activity was coeval with a period of extensional faulting, with minimal subsequent fault activity on the Crack in the Ground fault. The age of the Four Craters Lava Field is similar to the East lava field 6 km to the northwest. This illustrates the potential of cosmogenic dating to be applied to paleoseismic studies in extensional volcanic regions.

ACKNOWLEDGMENTS

Mackey conducted this research while a postdoctoral scholar at the California Institute of Technology and the University of Canterbury, and was partially supported by a Rutherford Foundation Postdoctoral Scholarship from the Royal Society of New Zealand. We thank Ken Farley and the Caltech Noble Gas Laboratory for helium analyses. Numerous University of Oregon geology field camps have mapped the Four Craters area, and provided motivation to establish the age of the lava field. We thank Rob Langridge for useful discussions, and the Bureau of Land Management for access to the site. Plots in Figure 5 were made from the Camelplot.m code written by Greg Balco. Comments by David Sherrod and an anonymous reviewer greatly improved the manuscript.

REFERENCES CITED

Akçar, N., Tikhomirov, D., Özkaymak, Ç., Ivy-Ochs, S., Alfimov, V., Sözbilir, H., Uzel, B., and Schlüchter, C., 2012, ^{36}Cl exposure dating of paleoearthquakes in the eastern Mediterranean: First results from the western Anatolian extensional province, Manisa fault zone, Turkey: Geological Society of America Bulletin, v. 124, p. 1724–1735, doi:10.1130/B30614.1.

Allison, I.S., 1979, Pluvial Fort Rock Lake, Lake County, Oregon: Oregon Department of Geology and Mineral Industries Special Paper 7, 72 p.

Amidon, W.H., and Farley, K.A., 2011, Cosmogenic ^{3}He production rates in apatite, zircon and pyroxene inferred from Bonneville flood erosional surfaces: Quaternary Geochronology, v. 6, p. 10–21, doi:10.1016/j.quageo.2010.03.005.

Balco, G., Stone, J.O., Lifton, N.A., and Dunai, T.J., 2008, A complete and easily accessible means of calculating surface exposure ages or erosion rates from ^{10}Be and ^{26}Al measurements: Quaternary Geochronology, v. 3, p. 174–195, doi:10.1016/j.quageo.2007.12.001.

Blard, P.H., and Farley, K.A., 2008, The influence of radiogenic ^{4}He on cosmogenic ^{3}He determinations in volcanic olivine and pyroxene: Earth and Planetary Science Letters, v. 276, p. 20–29, doi:10.1016/j.epsl.2008.09.003.

Brand, B.D., and Heiken, G., 2009, Tuff cones, tuff rings, and maars of the Fort Rock–Christmas Valley basin, Oregon: Exploring the vast array of pyroclastic features that record violent hydrovolcanism at Fort Rock and the Table Rock Complex, *in* O'Connor, J.E., et al., eds., Volcanoes to vineyards: Geologic field trips through the dynamic landscape of the Pacific Northwest: Geological Society of America Field Guide 15, p. 521–538, doi:10.1130/2009.fld015(25)

Cerling, T.E., and Craig, H., 1994, Cosmogenic ^{3}He production-rates from 39°N to 46°N latitude, western USA and France: Geochimica et Cosmochimica Acta, v. 58, p. 249–255, doi:10.1016/0016-7037(94)90462-6.

Crider, J.G., 2001, Oblique slip and the geometry of normal-fault linkage: Mechanics and a case study from the Basin and Range in Oregon: Journal of Structural Geology, v. 23, p. 1997–2009, doi:10.1016/S0191-8141(01)00047-5.

Desilets, D., Zreda, M., and Prabu, T., 2006, Extended scaling factors for in situ cosmogenic nuclides: New measurements at low latitude: Earth and Planetary Science Letters, v. 246, p. 265–276, doi:10.1016/j.epsl.2006.03.051.

Dunne, J.A., and Elmore, D., 2003, Monte Carlo simulations of low-energy cosmogenic neutron fluxes near the bottom of cliff faces: Earth and Planetary Science Letters, v. 206, p. 43–49, doi:10.1016/S0012-821X(02)01079-8.

Ely, L.L., and 11 others, 2012, Owyhee River intracanyon lava flows: Does the river give a dam?: Geological Society of America Bulletin, v. 124, p. 1667–1687, doi:10.1130/B30574.1.

Goehring, B.M., Kurz, M.D., Balco, G., Schaefer, J.M., Licciardi, J., and Lifton, N., 2010, A reevaluation of in situ cosmogenic ^{3}He production rates: Quaternary Geochronology, v. 5, p. 410–418, doi:10.1016/j.quageo.2010.03.001.

Graham, D.W., Reid, M.R., Jordan, B.T., Grunder, A.L., Leeman, W.P., and Lupton, J.E., 2009, Mantle source provinces beneath the northwestern USA delimited by helium isotopes in young basalts: Journal of Volcanology and Geothermal Research, v. 188, p. 128–140, doi:10.1016/j.jvolgeores.2008.12.004.

Gudmundsson, A., Brynjolfsson, S., and Jonsson, M.T., 1993, Structural analysis of a transform fault-rift zone junction in North Iceland: Tectonophysics, v. 220, p. 205–221, doi:10.1016/0040-1951(93)90232-9.

Hart, W.K., Aronson, J.L., and Mertzman, S.A., 1984, Areal distribution and age of low-K, high-alumina olivine tholeiite magmatism in the northwestern Great Basin: Geological Society of America Bulletin, v. 95, p. 186–195, doi:10.1130/0016-7606(1984)95<186:ADAAOL>2.0.CO;2.

Heiken, G.H., 1971, Tuff rings: Examples from the Fort Rock–Christmas Lake Valley Basin, south-central Oregon: Journal of Geophysical Research, v. 76, p. 5615–5626, doi:10.1029/JB076i023p05615.

Jordan, B.T., Grunder, A.L., Duncan, R.A., and Deino, A.L., 2004, Geochronology of age-progressive volcanism of the Oregon High Lava Plains: Implications for the plume interpretation of Yellowstone: Journal of Geophysical Research, v. 109, no. B10, B10202, doi:10.1029/2003JB002776.

Kuntz, M.A., Spiker, E.C., Rubin, M., Champion, D.E., and Lefebvre, R.H., 1986, Radiocarbon studies of latest Pleistocene and Holocene lava flows of the Snake River Plain, Idaho—Data, lessons, interpretations: Quaternary Research, v. 25, p. 163–176, doi:10.1016/0033-5894(86)90054-2.

Kurz, M.D., 1986, In situ production of terrestrial cosmogenic helium and some applications to geochronology: Geochimica et Cosmochimica Acta, v. 50, p. 2855–2862, doi:10.1016/0016-7037(86)90232-2.

Licciardi, J.M., Kurz, M.D., Clark, P.U., and Brook, E.J., 1999, Calibration of cosmogenic ^{3}He production rates from Holocene lava flows in Oregon, USA, and effects of the Earth's magnetic field: Earth and Planetary Science Letters, v. 172, p. 261–271, doi:10.1016/S0012-821X(99)00204-6.

Mackey, B.H., Scheingross, J.S., Lamb, M.P., and Farley, K.A., 2014, Knickpoint formation, rapid propagation, and landscape response following coastal cliff retreat at the last interglacial sea-level highstand: Kaua'i, Hawai'i: Geological Society of America Bulletin, v. 126, p. 925–942, doi:10.1130/B30930.1.

Margerison, H.R., Phillips, W.M., Stuart, F.M., and Sugden, D.E., 2005, Cosmogenic ^{3}He concentrations in ancient flood deposits from the Coombs Hills, northern Dry Valleys, East Antarctica: Interpreting exposure ages and erosion rates: Earth and Planetary Science Letters, v. 230, p. 163–175, doi:10.1016/j.epsl.2004.11.007.

Matmon, A., Shaked, Y., Porat, N., Enzel, Y., Finkel, R., Lifton, N., Boaretto, E., and Agnon, A., 2005, Landscape development in an hyperarid sandstone environment along the margins of the Dead Sea fault: Implications from dated rock falls: Earth and Planetary Science Letters, v. 240, p. 803–817, doi:10.1016/j.epsl.2005.06.059.

Meigs, A., and 13 others, 2009, Geological and geophysical perspectives on the magmatic and tectonic development, High Lava Plains and northwest Basin and Range, *in* O'Connor, J.E., et al., eds., Volcanoes to vineyards: Geologic field trips through the dynamic landscape of the Pacific Northwest: Geological Society of America Field Guide 15, p. 435–470, doi:10.1130/2009.fld015(21).

Peterson, N.V., and Groh, E.A., 1963, Recent volcanic landforms in Central Oregon: The Ore Bin, v. 25, no. 3, p. 33–45.

Peterson, N.V., and Groh, E.A., 1964, Crack-In-The-Ground, Lake County, Oregon: The Ore Bin, v. 26, no. 9, p. 158–166.

Pezzopane, S.K., and Weldon, R.J., 1993, Tectonic role of active faulting in central Oregon: Tectonics, v. 12, p. 1140–1169, doi:10.1029/92TC02950.

Rinat, Y., Matmon, A., Arnold, M., Aumaître, G., Bourlès, D., Keddadouche, K., Porat, N., Morin, E., and Finkel, R.C., 2014, Holocene rockfalls in the southern Negev Desert, Israel and their relation to Dead Sea fault earthquakes: Quaternary Research, v. 81, p. 260–273, doi:10.1016/j.yqres.2013.12.008.

Schlagenhauf, A., Manighetti, I., Benedetti, L., Gaudemer, Y., Finkel, R., Malavieille, J., and Pou, K., 2011, Earthquake supercycles in central Italy, inferred from ^{36}Cl exposure dating: Earth and Planetary Science Letters, v. 307, p. 487–500, doi:10.1016/j.epsl.2011.05.022.

Sherrod, D.R., Champion, D.E., and McGeehin, J.P., 2012, Age and duration of volcanic activity at Diamond Craters, southeastern Oregon: Journal of Volcanology and Geothermal Research, v. 247, p. 108–114, doi:10.1016/j.jvolgeores.2012.08.008.

Sims, K.W.W., Ackert, R.P., Ramos, F.C., Sohn, R.A., Murrell, M.T., and DePaolo, D.J., 2007, Determining eruption ages and erosion rates of Quaternary basaltic volcanism from combined U-series disequilibria and cosmogenic exposure ages: Geology, v. 35, p. 471–474, doi:10.1130/G23381A.1.

Tibaldi, A., 1995, Morphology of pyroclastic cones and tectonics: Journal of Geophysical Research, v. 100, no. B12, p. 24521–24535, doi:10.1029/95JB02250.

Walker, G.W., and MacLeod, N.S., 1991, Geologic map of Oregon: U.S. Geological Survey, scale 1:500,000.

Walker, G.W., Peterson, N.V., and Greene, R.C., 1967, Reconnaissance geologic map of the east half of the Crescent quadrangle, Lake, Deschutes, and Crook Counties, Oregon: U.S. Geological Survey Miscellaneous Geologic Investigations Map I-493, scale 1:250,000, http://ngmdb.usgs.gov/Prodesc/proddesc_1708.htm.

Weldon, R.J., Fletcher, D.K., Weldon, E.M., Scharer, K.M., and McCrory, P.A., 2003, An update of Quaternary faults of central and eastern Oregon: U.S. Geological Survey Open-File Report 02-301, 26 map sheets, scale 1:100,000, CD-ROM, http://pubs.usgs.gov/of/2002/of02-301/.

Zdanowicz, C.M., Zielinski, G.A., and Germani, M.S., 1999, Mount Mazama eruption: Calendrical age verified and atmospheric impact assessed: Geology, v. 27, p. 621–624, doi:10.1130/0091-7613(1999)027<0621:MMECAV>2.3.CO;2.

Geosphere

Synchronous late Pleistocene extensional faulting and basaltic volcanism at Four Craters Lava Field, central Oregon, USA

Benjamin H. Mackey, Samuel R. Castonguay, Paul J. Wallace and Ray J. Weldon

Geosphere 2014;10;1247-1254
doi: 10.1130/GES00990.1

Notes